JOURNAL OF AGRICULTURAL AND FOOD CHEMISTRY

Investigation of Adsorption Behavior of (−)-Epigallocatechin Gallate on Bovine Serum Albumin Surface Using Quartz Crystal Microbalance with Dissipation Monitoring

XIAOYONG WANG, CHI-TANG HO, AND QINGRONG HUANG*

Department of Food Science, Rutgers University, 65 Dudley Road, New Brunswick, New Jersey 08901

Quartz crystal microbalance with dissipation monitoring (QCM-D) has been employed to study the interactions between (−)-epigallocatechin gallate (EGCG) and bovine serum albumin (BSA) surface. The adsorbed mass, thickness, and viscoelastic properties of EGCG adlayer on BSA surface at various EGCG concentrations, temperatures, sodium chloride concentrations, and pH values have been determined by QCM-D in combination with the Voigt model. The adsorption isotherm of EGCG on BSA surfaces can be better described by the Freundlich model than the Langmuir model, indicating that EGCG adsorption on BSA surfaces is dominated by nonspecific hydrophobic interactions, as supported by stronger EGCG adsorption at higher temperature. Shifts in the Fourier transform infrared spectra of the BSA surface with and without EGCG adsorption disclose that hydrogen bonding might also be involved in EGCG adsorption on BSA surfaces. The addition of salt and change of pH can also influence the EGCG adsorption on BSA surfaces. Usually, higher EGCG adsorption leads to higher values of viscosity and shear elastic modulus of EGCG adlayer, which can be explained by the aggregation of BSA through EGCG bridges. Compared with EGCG, nongalloylated (+)-catechin shows much lower adsorption capacity on BSA surfaces, suggesting the importance of the galloyl group in polyphenol/protein interactions.

KEYWORDS: (−)-Epigallocatechin gallate; bovine serum albumin; interfacial interaction; mass, viscoelastic properties; hydrophobic interaction; hydrogen bonding; galloyl group

INTRODUCTION

Green tea has become one of the most popular beverages in the world in recent years, primarily because of its beneficial biological and pharmacological effects, including antioxidant, antimutagenic, anticarcinogenic, antiviral, antiinflammatory, and anticancer activities, which have been demonstrated in numerous human, animal, and in vivo studies (*1*−*6*). These antidisease effects are most often attributed to green tea catechins, the typical polyphenols contained in green tea that include (+)-catechin, (−)-epicatechin, (−)-epicatechin gallate, and (−)-epigallocatechin gallate (EGCG). Among these polyphenols, epidemiological and experimental studies in animals and human suggest that EGCG is the most effective one (*7*, *8*). It is well-known that polyphenols can associate with proteins to form soluble and insoluble complexes, leading to various unfavorable consequences, such as impairment of polyphenol absorption (*9*), reduction of health-promotion potential (*10*), sensation of astringency in the mouth (*11*), limitation of beverage quality (*12*), and even fouling of process equipment surfaces (*13*). Improved insights into the molecular basis of interactions between polyphenols and proteins should, therefore, help to better control the health activities of polyphenols and improve the actual effectiveness of beverages.

Various techniques, including light scattering (*14*), fluorescence (*15*), and size exclusion chromatography (*16*), disclose that non-electrostatic interactions, such as hydrophobic interactions and hydrogen bonding, are the main driving forces of the interactions between polyphenols and proteins in solution. The nature of the interactions also depends upon pH, temperature, solvent, and protein and polyphenol structures (*17*, *18*). Possibly due to both the complexity of experimental design and the lack of highly sensitive techniques, little is known about the interactions of polyphenols and proteins at the liquid/solid interface, even though they are often seen in actual biological and industrial processes. Recently, quartz crystal microbalance with dissipation monitoring (QCM-D), traditionally used in the laboratories of analytical and electroanalytical chemistries, has become a powerful technique to study various biological surface science-related phenomena (*19*, *20*). On the basis of the piezoelectric effect, QCM-D can simultaneously determine changes in the frequency (ΔF) and the energy dissipation (ΔD) of a quartz crystal at nanoscale in real time. This enables QCM-D to determine not only the mass and thickness of adlayers but also the viscoelastic properties of surface-bound molecules (*21*).

* Author to whom correspondence should be addressed [telephone 732-932-7193; fax (732) 932-6776; e-mail qhuang@aesop.rutgers.edu].

10.1021/jf070590l CCC: $37.00
Published on Web 05/31/2007

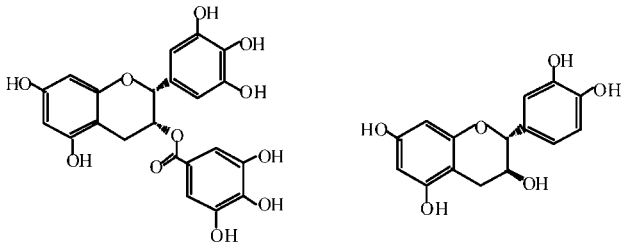

(−)-Epigallocatechin gallate (+)-Catechin

Figure 1. Structures of EGCG and (+)-catechin.

In this paper, QCM-D is used to study the interactions between EGCG and bovine serum albumin (BSA) surfaces, wherein BSA is chemically immobilized on the gold-coated quartz crystal. The adsorbed mass, thickness, and viscoelastic properties of the EGCG adlayer on BSA surface at various EGCG concentrations, temperatures, sodium chloride concentrations, and pH values are determined by a combination of QCM-D and the Voigt model. In addition, the adsorption behavior of (+)-catechin on BSA surface is also investigated to see the role of polyphenol structure in polyphenol/protein interactions.

MATERIALS AND METHODS

Materials. BSA (≥98% pure by gel electrophoresis) was purchased from Sigma Chemical Co. and used without further purification. EGCG (≥95%) and (+)-catechin (≥98%) were purchased from DSM (Basel, Switzerland) and Sigma Chemical Co., respectively. The chemical structures of EGCG and (+)-catechin are depicted in **Figure 1**. 11-Mercaptoundecanoic acid (11-MUA) (Aldrich), *N*-hydroxysuccinimide (NHS) (Aldrich), 1-ethyl-3-(3-dimethylaminopropyl)carbodiimide hydrochloride (EDC) (Sigma), acetic acid (Aldrich), sodium acetate (Fisher), ammonium hydroxide (NH_4OH) (VWR), hydrogen peroxide (H_2O_2) (Aldrich), sodium chloride (NaCl) (Fisher), and absolute ethanol (Fisher) were all used as received. The buffers used were 0.005 M phosphate buffer at pH 7.0 and 0.010 M sodium acetate buffers at pH 4.9 and 3.0.

Preparation of BSA Surface. AT-cut quartz crystal coated with gold (fundamental frequency of 5 MHz) was obtained from Q-Sense AB (Västra Frölunda, Sweden). The linkage of BSA onto the gold-coated crystal was produced using a procedure modified from a previous paper (*22*). Gold-coated quartz crystal were first cleaned in a UV/ozone chamber for 10 min, followed by immersion in a 1:1:5 mixture of ammonium hydroxide (NH_4OH, 25%), hydrogen peroxide (H_2O_2, 30%), and Milli-Q water for 5 min at 75 °C, and finally cleaned in a UV/ozone chamber for another 10 min. These gold-coated crystals were then rinsed with a large quantity of Milli-Q water, dried with nitrogen gas (N_2), and subsequently soaked in 10 mM 11-MUA in absolute ethanol at 60 °C for at least 24 h. The excess amount of 11-MUA was rinsed off with absolute ethanol, and the modified quartz crystal surfaces were dried under N_2 flow. Just before the immobilization of protein, 11-MUA-coated quartz crystal surfaces were activated by a mixed solution containing 1:1 (v/v) 100 mg/mL EDC and 100 mg/mL NHS in Milli-Q water for 1 h. A solution of 10 mg/mL BSA in phosphate buffer (pH 7.0) was used to incubate the activated surfaces at 4 °C for at least 24 h. Finally, the quartz crystal surfaces were rinsed with phosphate buffer followed by Milli-Q water and dried under N_2 flow.

Grazing Angle FTIR. Infrared spectra of BSA-modified quartz crystal surfaces both before and after EGCG adsorption were collected with a Fourier transform infrared spectrometer (Thermo Nicolet 670, Madison, WI), using a pure gold surface as the background. A Thermo Nicolet smart apertured grazing angle (SAGA) accessory with a grazing angle of incidence of 80° was used to collect reflection absorption infrared spectra. The resolution was set to 4 cm^{-1}, and 1024 scans were collected.

QCM-D Measurements. The interactions between polyphenols and BSA chemically linked quartz crystal surface were studied using a commercial QCM-D apparatus (Q-Sense AB) with a Q-Sense D300 electronic unit. A polypropylene pipet tip connecting to the temperature-controlled chamber was initially filled with buffers of various pH values and sodium chloride concentrations (C_{NaCl}). By opening the valve, buffer solutions were exchanged in the QCM-D chamber via gravitational flow. After a stable baseline was established, polyphenol solutions in buffers of the same pH and C_{NaCl} were exposed to BSA-modified crystal surfaces. At the same time, the adsorption was monitored, as a function of time, by simultaneously recording the shifts in the frequency (ΔF) and in the energy dissipation (ΔD) at the fundamental resonant frequency, along with the third, fifth, and seventh overtones, until a steady state of adsorption was reached, where the long-term stability of the frequency was within 1 Hz, which was negligible when compared with the frequency shifts due to adsorption. Normalized data obtained from different overtones were used in the calculation of mass load, thickness, and viscoelastic properties of adsorbed layers using the Voigt model. Sauerbrey mass was calculated using the Sauerbrey equation (*23*):

$$M = -(C/n)\Delta F \quad (1)$$

ΔF, M, and n represent frequency change, adsorbed mass per unit area, and overtone number, respectively. C is the mass sensitivity constant (17.7 ng/cm^{2}Hz). Q-Sense software determines the resonance frequency and the decay time, τ_0, of the exponentially damped sinusoidal voltage signal over the crystal, and the dissipation factor, D, can be obtained from equation

$$D = \frac{1}{\pi f_0 \tau_0} = \frac{2}{\omega \tau_0} \quad (2)$$

where f_0 is the resonance frequency and τ_0 is the decay time.

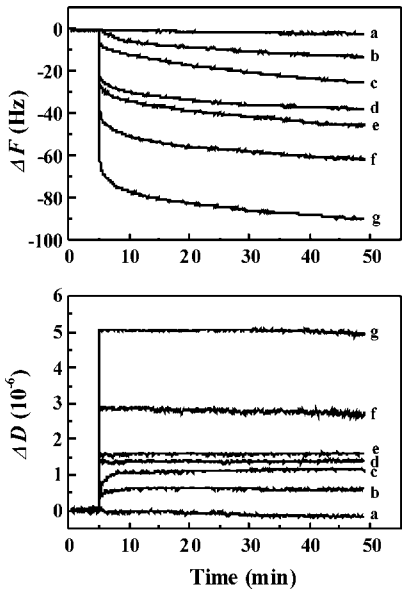

Figure 2. Time-dependent frequency shifts and energy dissipation shifts for EGCG adsorption on BSA-modified quartz crystal surfaces at various EGCG concentrations: (a) C_{EGCG} = 1 mM; (b) C_{EGCG} = 5 mM; (c) C_{EGCG} = 10 mM; (d) C_{EGCG} = 15 mM; (e) C_{EGCG} = 20 mM; (f) C_{EGCG} = 30 mM; (g) C_{EGCG} = 50 mM.

RESULTS AND DISCUSSION

Figure 2 displays the typical time-resolved resonance frequency shifts (ΔF) and energy dissipation shifts (ΔD) for the third overtone upon the addition of various concentrations of EGCG onto BSA surface using pH 4.9 sodium acetate buffers without the addition of sodium chloride at 25 °C. Prior to the introduction of EGCG solution into the chamber, a steady baseline was acquired. Immediately after the injection of each

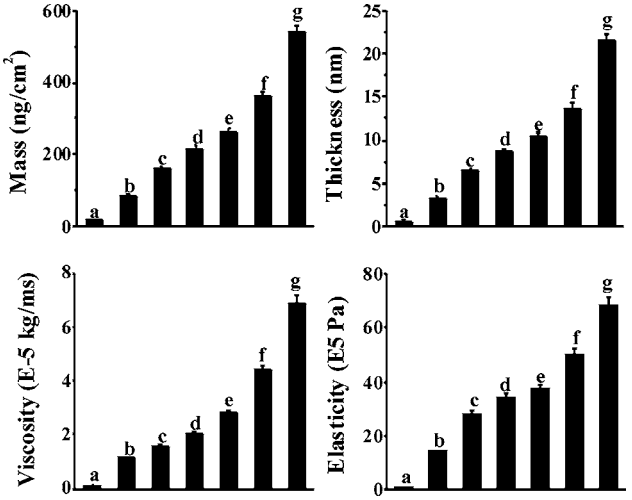

Figure 3. Changes of mass, thickness, viscosity, and shear elastic modulus of EGCG adlayer on BSA surfaces at various EGCG concentrations: (a) $C_{EGCG} = 1$ mM; (b) $C_{EGCG} = 5$ mM; (c) $C_{EGCG} = 10$ mM; (d) $C_{EGCG} = 15$ mM; (e) $C_{EGCG} = 20$ mM; (f) $C_{EGCG} = 30$ mM; (g) $C_{EGCG} = 50$ mM.

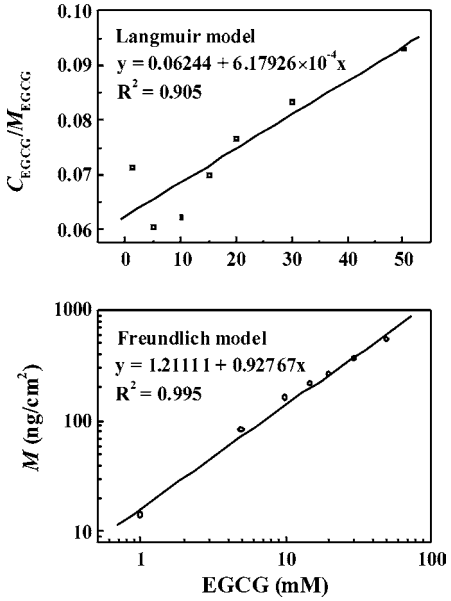

Figure 4. Adsorption isotherm of EGCG onto BSA surfaces fitted to the Langmuir model (top) and the Freundlich model (bottom).

EGCG solution, there was often a rapid decrease in ΔF and a marked increase in ΔD, followed by much more gradual changes of ΔF and ΔD until steady states were reached (i.e., the frequency shift was within 1 Hz). These changes in ΔF and ΔD indicate the adsorption of EGCG on BSA surface. Software (QTools), based on the Voigt model, was used to model the responses at the third, fifth, and seventh overtones during the process of EGCG adsorption on BSA surfaces, to provide the mass, thickness, viscosity, and elastic shear modulus of the adsorbed EGCG adlayer on BSA surfaces, as shown in **Figure 3**.

The adsorption isotherm of EGCG onto BSA surfaces can be determined from the changes of the adsorbed EGCG mass against EGCG concentration. The Langmuir model assumes the monolayer coverage of adsorbate over a homogeneous adsorbent surface, and a saturation point is finally reached according to the equations (*24*)

$$M = \frac{M_m KC}{1 + KC} \tag{3}$$

$$\frac{C}{M} = \frac{1}{KM_m} + \frac{1}{M_m}C \tag{4}$$

where C is the concentration of adsorbate solution, M is the amount of adsorbate on the adsorbent, K is a direct measure of the intensity of the adsorption process, and M_m is a constant related to the area occupied by a monolayer of adsorbate, reflecting the adsorption capacity. However, the experimental data of EGCG adsorption on BSA surfaces have an unsatisfactory fit to the Langmuir model, as shown in **Figure 4**, indicating that the Langmuir model is not ideal for EGCG adsorption behavior. In fact, the increasing tendency of the mass/thickness of EGCG adlayer without a concomitant saturation as EGCG concentration increases (as seen in **Figure 3**) also weakens the assumption of monolayer adsorption in the Langmuir model. We then turned to the Freundlich model, an empirical exponential equation, which assumes that the mass of adsorbates on the adsorbent surface increases as the adsorbate concentration increases (*25*). The Freundlich equation can be expressed as

$$M = K_f C^{1/n} \tag{5}$$

where n and K_f are constants and C is the EGCG concentration of the solution. Its logarithmic form is

$$\log M = \log K_f + 1/n \log C \tag{6}$$

Figure 4 presents the close relationship between the Freundlich model and the data of EGCG adsorption on BSA surfaces, with a correlation coefficient of 0.995. The correspondence of the EGCG adsorption isotherm to the Freundlich model rather than to the Langmuir model disproves the formation of a "simple" EGCG monolayer on the BSA surface. Some adsorbed EGCG molecules may act as bridges (*14*) to let BSA molecules aggregate with each other. At the same time, water, coupled with BSA molecules (*26*), will be gradually driven out during the EGCG adsorption. Consequently, the higher mass of EGCG adsorbed on the BSA surface will cause an increase in both viscosity and shear elastic modulus of the EGCG adlayer, as shown by the higher values of viscosity and shear elastic modulus of the EGCG adlayer at higher EGCG adsorbed mass (shown in **Figure 3**). The better fitting of the Freundlich model also indicates that EGCG adsorption onto the BSA surface may mainly be governed by nonspecific hydrophobic interactions, in agreement with previous studies of polyphenol/protein interactions in solutions (*11*). BSA is a globular protein composed of three structurally similar domains (I, II, and III), each containing a number of hydrophobic cavities (*27*). In particular, there are two hydrophobic sites located in subdomains IIA and IIIA. When EGCG solution is added, hydrophobic EGCG can bind to the BSA surface through hydrophobic interaction. A higher concentration of the EGCG solution leads to a larger amount of EGCG molecules adsorbed on the BSA surface, resulting in a greater increase in the mass/thickness of the EGCG adlayer.

The dominant hydrophobic interaction during EGCG adsorption onto a BSA surface can be verified by temperature-dependent QCM-D measurements for 20 mM EGCG at 25, 30, and 35 °C, as shown in **Figure 5**, where the higher mass of the

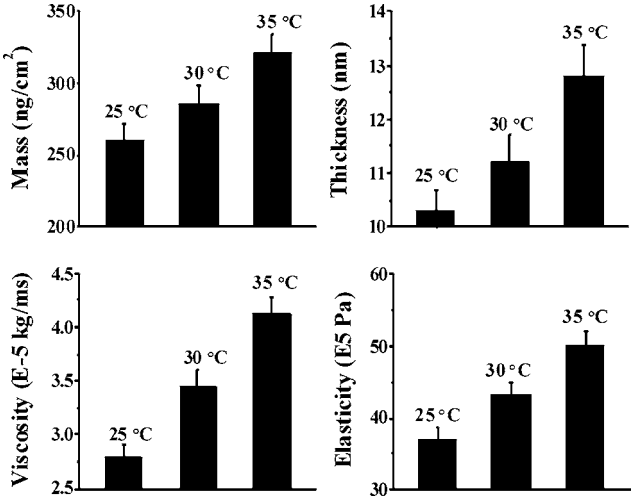

Figure 5. Changes of mass, thickness, viscosity, and shear elastic modulus of EGCG adlayer on BSA surfaces for 20 mM EGCG adsorption at various temperatures.

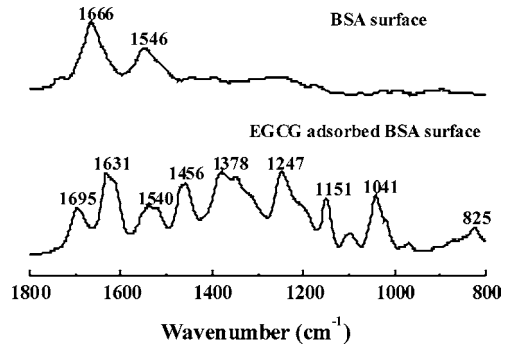

Figure 6. FTIR spectra of pure BSA surface (top) and BSA surfaces with adsorbed EGCG (bottom).

EGCG adlayer was observed at the higher temperature. Below the critical denaturing temperature of BSA (i.e., 60 °C) (*28*), increasing temperature causes partial unfolding of BSA molecules, which in turn increases the exposure of the hydrophobic surfaces of the protein, to which more EGCG molecules can bind. The driving force for hydrophobic EGCG/BSA interaction may be attributed to the relatively nonpolar structure of EGCG. It was proposed that polyphenol polarity determined whether the polyphenol/protein interaction was mediated via hydrophobic force or hydrogen bonding (*29*). Because of the stronger EGCG adsorption at higher temperatures, both the viscosity and shear elastic modulus of the EGCG adlayer are observed to have larger values when the temperature increases from 25 to 35 °C.

Owing to their proton-donating potential, the hydroxyl groups existing in EGCG may form hydrogen bonds with H-acceptor sites in BSA (*30*). To know whether hydrogen bonding is involved in EGCG adsorption, FTIR spectra of the BSA surface with and without the adsorption of 20 mM EGCG were recorded, as shown in **Figure 6**. The FTIR spectrum of a pure BSA surface displays two characteristic bands, at 1666 and 1546 cm^{-1}. The 1666 cm^{-1} (amide I) band arises predominantly from protein amide C═O stretching vibrations, and the 1546 cm^{-1} (amide II) band is due to the amide N—H bending vibrations and C—N stretching vibrations (*31*). The position of the amide band I on the EGCG adsorbed BSA surface has a remarkable shift from 1666 to 1631 cm^{-1}. The amide II band has a relatively smaller change, from 1546 to 1540 cm^{-1}, after EGCG adsorption. New peaks at 1695, 1456, 1378, 1247, 1151, 1041, and 825 cm^{-1} in the IR spectra of EGCG adsorbed BSA surfaces

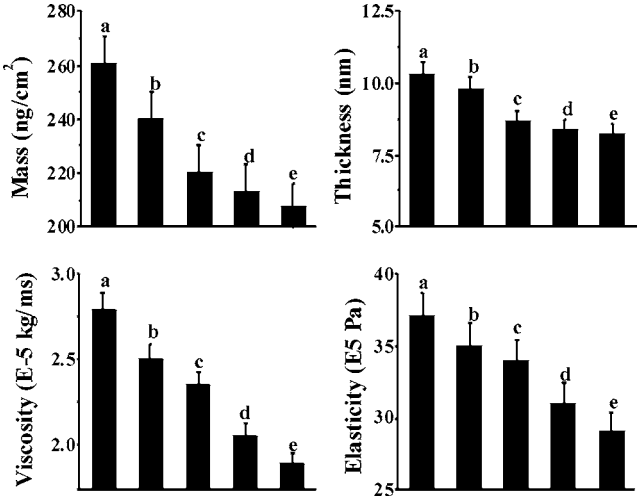

Figure 7. Changes of mass, thickness, viscosity, and shear elastic modulus of EGCG adlayer on BSA surfaces for 20 mM EGCG adsorption at various sodium chloride concentrations: (a) C_{NaCl} = 0 M; (b) C_{NaCl} = 0.01 M; (c) C_{NaCl} = 0.03 M; (d) C_{NaCl} = 0.05 M; (e) C_{NaCl} = 0.1 M.

are observed, which show the characteristic bands of EGCG (*32*). Although EGCG bridges may cause somewhat BSA aggregation, hydrogen bonding between the phenolic hydroxyl groups of EGCG and the amide groups of BSA may also occur and is mainly responsible for the peak position changes in the amide I and amide II bands.

Figure 7 shows the changes of mass, thickness, viscosity, and shear elastic modulus of the EGCG adlayer on BSA surfaces for 20 mM EGCG at different sodium chloride concentrations. EGCG adsorption onto BSA surfaces is sensitive to salt concentration, with a 20% decrease in the adsorbed mass when C_{NaCl} increases from 0 to 0.1 M. The present salt-reduced effect seems contrary to our above conclusion regarding the dominant hydrophobic interaction in EGCG/BSA interaction, because the addition of salt usually enhances the hydrophobic interaction. This disagreement may be explained as follows: At the investigated pH value of 4.9, close to the isoelectric point (p*I*) of BSA, protein molecules still have very low surface charges. It has been reported that BSA molecules near their p*I* are capable of self-association through the electrostatic interactions between positively and negatively charged patches on their surface. The addition of small amounts of metal ions (i.e., <0.2 M) can weaken the attraction between the protein molecules and let BSA molecules exist as monomers (*33*). The decrease in protein molecular size may not only suppress EGCG adsorption but also inhibit the EGCG bridge function for BSA aggregation due to the existence of a certain critical distance for the formation of the interprotein complexes. Therefore, it is observed that increasing salt concentration leads to less EGCG adsorption and lower values of viscosity and shear elastic modulus of EGCG adlayer.

Besides the experiments done at pH 4.9, QCM-D measurements were also conducted at pH 7.0 and 3.0, at which BSA carries negative and positive charges, respectively. The mass, thickness, viscosity, and elastic shear modulus of the adsorbed EGCG adlayer on BSA surface for 20 mM EGCG adsorption at pH 7.0, 4.9, and 3.0 are compared in **Figure 8**. The significantly higher adsorbed EGCG mass at pH 4.9 than at pH 7.0 and 3.0 supports the main hydrophobic interaction in EGCG adsorption on the BSA surface. The maximum binding of a protein by polyphenols at pH near the p*I* has also been reported by other investigators (*34*, *35*). The higher protein charges are

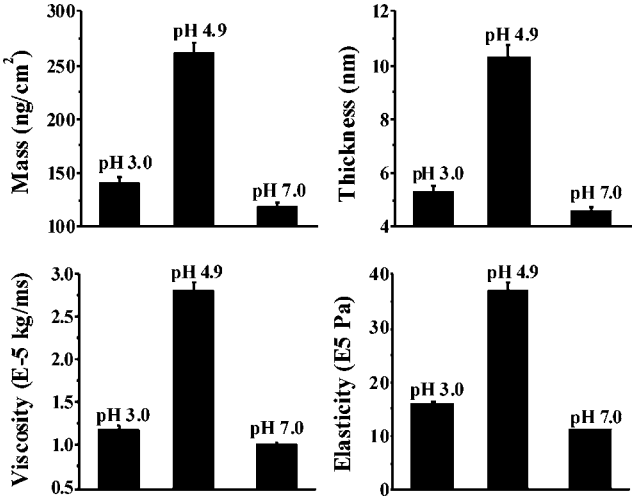

Figure 8. Changes of mass, thickness, viscosity, and shear elastic modulus of EGCG adlayer on BSA surfaces for 20 mM EGCG adsorption at various pH values.

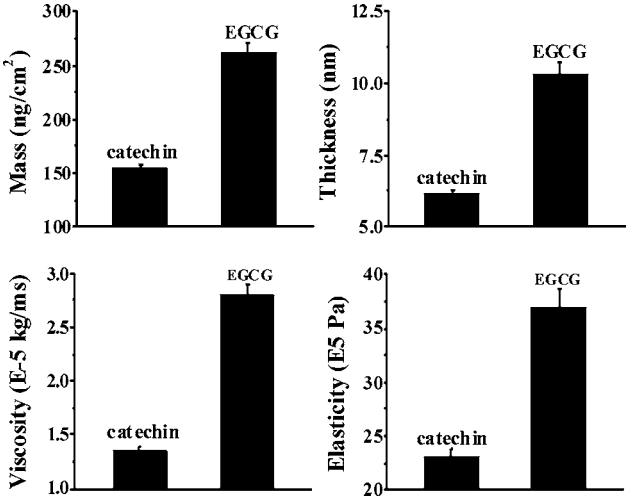

Figure 9. Comparison of mass, thickness, viscosity, and shear elastic modulus of EGCG adlayer with (+)-catechin adlayer on BSA surfaces (C_{EGCG} = 20 mM, $C_{catechin}$ = 20 mM).

responsible for the lower EGCG adsorption capacities at both pH 7.0 and 3.0, leading to smaller values of viscosity and shear elastic modulus of EGCG adlayer at either of these two pH values than that at pH 4.9. It should be noted that more EGCG is found to be adsorbed to BSA surfaces at pH 3.0 than at pH 7.0. BSA is known to undergo conformational isomerization by decreasing pH, beginning with the heart-shaped normal "*N*" form at neutral pH, followed by the fast "*F*" form (40 × 129 Å) below a pH of about 4.0, and concluding with the expanded "*E*" form (21 × 250 Å) for pH less than about 3.0 (*36*). The more open conformation of BSA structure at pH 3.0 than at pH 7.0 possibly results in a higher affinity for EGCG molecules.

Many experiments have shown that the catechins with a galloyl moiety, such as EGCG, are more effective in biological activities than their homologues lacking the galloyl group (*37*). The interaction between polyphenol and protein was observed to be enhanced with the increasing number of galloyl groups (*38*), which could increase the conformational mobility of polyphenol and thus maximize the polyphenol/protein interactions. To study the role of the galloyl moiety, QCM-D has also been employed to measure the binding of 20 mM (+)-catechin without galloyl group on BSA surfaces at pH 4.9. **Figure 9** shows that the values of mass, thickness, viscosity, and shear elastic modulus of the EGCG adlayer are higher than those of the (+)-catechin adlayer. When one is dealing with nongalloylated (+)-catechin, there are two phenolic rings involved in the hydrophobic interaction with BSA surfaces. In contrast, three phenolic rings are involved in the binding with BSA surfaces in the case of EGCG. As a result, EGCG molecules have more phenolic groups capable of binding to BSA surfaces through the hydrophobic interaction without any major conformational restriction. Moreover, the stronger adsorption of EGCG on BSA surfaces than of (+)-catechin may partially originate from the larger number of phenolic hydroxyl groups in EGCG that may cause stronger hydrogen bonding with BSA.

In conclusion, hydrophobic interaction is the main driving force for EGCG adsorption on BSA surfaces, as indicated by the better fitting of the Freundlich model than the Langmuir model, as well as the temperature-promoted EGCG adsorption. EGCG adsorption on BSA surfaces is significantly affected by the addition of salt and the variation of pH. The unique viscoelastic properties of EGCG adlayers provided by QCM-D suggest that higher EGCG adsorption favors the formation of a more compact adlayer with higher viscosity and shear elastic modulus owing to the aggregation of BSA through EGCG bridges.

LITERATURE CITED

(1) Valcic, S.; Muders, A.; Jacobsen, N. E.; Liebler, D. C.; Timmermann, B. N. Antioxidant chemistry of green tea catechins. Identification of products of the reaction of (−)-epigallocatechin gallate with peroxyl radicals. *Chem. Res. Toxicol.* **1999**, *12*, 382−386.

(2) Price, W. E. Green tea flavanols and cancer. *Agro-Food Ind. Hi-Tech.* **1994**, *5* (Sept/Oct), 18−20.

(3) Wang, Z. Y.; Huang, M. T.; Lou, Y. R.; Xie, J. G.; Reuhl, K. R.; Newmark, H. L.; Ho, C. T.; Yang, C. S.; Conney, A. H. Inhibitory effects of black tea, green tea, decaffeinated black tea, and decaffeinated green tea on ultraviolet B light-induced skin carcinogenesis in 7,12-dimethylbenz[*a*]anthracene-initiated SKH-1 mice. *Cancer Res.* **1994**, *54*, 3428−3435.

(4) John, T. J.; Mukundan, P. Antiviral property of tea. *Curr. Sci.* **1978**, *47*, 159−160.

(5) Middleton, Jr., E.; Kandaswami, C.; Theoharides, T. C. The effects of plant flavonoids on mammalian cells: implications for inflammation, heart disease, and cancer. *Pharmacol. Rev.* **2000**, *52*, 673−751.

(6) Jankun, J.; Selman, S. H.; Swiercz, R.; Skrzypczak-Jankun, E. Why drinking green tea could prevent cancer. *Nature* **1997**, *387*, 561.

(7) Higdon, J. V.; Frei, B. Tea catechins and polyphenols: health effects, metabolism, and antioxidant functions. *Crit. Rev. Food Sci. Nutr.* **2003**, *43*, 89−143.

(8) Stuart, E. C.; Scandlyn, M. J.; Rosengren, R. J. Role of epigallocatechin gallate (EGCG) in the treatment of breast and prostate cancer. *Life Sci.* **2006**, *79*, 2329−2336.

(9) Riedl, K. M.; Hagerman, A. E. Tannin−protein complexes as radical scavengers and radical sinks. *J. Agric. Food Chem.* **2001**, *49*, 4917−4923.

(10) Arts, M. J. T. J.; Haenen, G. R. M. M.; Wilms, L. C.; Beetstra, S. A. J. N.; Heijnen, C. G. M.; Voss, H.-P.; Bast, A. Interactions between flavonoids and proteins: effect on the total antioxidant capacity. *J. Agric. Food Chem.* **2002**, *50*, 1184−1187.

(11) Jöbstl, E.; O'Connell, J.; Fairclough, J. P. A.; Williamson, M. P. Molecular model for astringency produced by polyphenol/protein interactions. *Biomacromolecules* **2004**, *5*, 942−949.

(12) O'Connell, J. E.; Fox, P. F. Significance and applications of phenolic compounds in the production and quality of milk and dairy products: a review. *Int. Dairy J.* **2001**, *11*, 103−120.

(13) Eagles, W. P.; Wakeman, R. J. Interactions between dissolved material and the fouling layer during microfiltration of a model beer solution. *J. Membr. Sci.* **2002**, *206*, 253−264.
(14) Siebert, K. J.; Troukhanova, N. V.; Lynn, P. Y. Nature of polyphenol−protein interactions. *J. Agric. Food Chem.* **1996**, *44*, 80−85.
(15) Dufour, C.; Dangles, O. Flavonoid−serum albumin complexation: determination of binding constants and binding sites by fluorescence spectroscopy. *Biochim. Biophys. Acta* **2005**, *1721*, 164−173.
(16) Hatano, T.; Hori, M.; Hemingway, R. W.; Yoshida, T. Size exclusion chromatographic analysis of polyphenol−serum albumin complexes. *Phytochemistry* **2003**, *63*, 817−823.
(17) Luck, G.; Liao, H.; Murray, J.; Grimmer, H.; Warminski, E.; Williamson, M.; Lilley, E. H.; Haslam, E. Polyphenols, astringency and proline-rich proteins. *Phytochemistry* **1994**, *37*, 357−371.
(18) Siebert, K. J. Effects of protein−polyphenol interactions on beverage haze, stabilization, and analysis. *J. Agric. Food Chem.* **1999**, *47*, 353−362.
(19) Janshoff, A.; Galla, H. J.; Steinem, C. Piezoelectric mass-sensing devices as biosensors—an alternative to optical biosensors? *Angew. Chem., Int. Ed.* **2000**, *39*, 4004−4032.
(20) Marx, K. A. Quartz crystal microbalance: a useful tool for studying thin polymer films and complex biomolecular systems at the solution-surface interface. *Biomacromolecules* **2003**, *4*, 1099−1120.
(21) Weber, N.; Wendel, H. P.; Kohn, J. Formation of viscoelastic protein layers on polymeric surfaces relevant to platelet adhesion. *J. Biomed. Mater. Res. A* **2005**, *72*, 420−427.
(22) Patel, N.; Davies, M. C.; Heaton, R. J.; Roberts, C. J.; Tendler, S. J. B.; Williams, P. A scanning probe microscopy study of the physisorption and chemisorption of protein molecules onto carboxylate terminated self-assembled monolayers. *Appl. Phys. A* **1998**, *66*, S569−S574.
(23) Sauerbrey, G. Verwendung von schwingquarzen zur wägung dünner schichten und zur mikrowägung (The use of quartz oscillators for weighing thin layers and for microweighing). *ZPhys−e.A: Hadrons Nucl.* **1959**, *155*, 206−222.
(24) Langmuir, I. The adsorption of gases on plane surfaces of glass, mica and platinum. *J. Am. Chem. Soc.* **1918**, *40*, 1361−1403.
(25) Parfitt, G. D., Rochester, C. H., Eds. *Adsorption from Solution at Solid/Liquid Interfaces*; Academic Press: London, U.K., 1983.
(26) Höök, F.; Kasemo, B.; Nylander, T.; Fant, C.; Sott, K.; Elwing, H. Variations in coupled water, viscoelastic properties, and film thickness of a mefp-1 protein film during adsorption and cross-linking: a quartz crystal microbalance with dissipation monitoring, ellipsometry, and surface plasmon resonance study. *Anal. Chem.* **2001**, *73*, 5796−5804.
(27) Foster, J. F. Some aspects of the structure and conformational properties of serum albumin. In *Albumin Structure, Function and Uses*; Rosenoer, V. M., Oratz, M., Rothschild, M. A., Eds.; Pergamon Press: Oxford, U.K., 1977; pp 53−84.
(28) Takeda, K.; Wada, A.; Yamamoto, K.; Moriyama, Y.; Aoki, K. Conformational change of bovine serum albumin by heat treatment. *J. Protein Chem.* **1989**, *8*, 653−659.
(29) Hagerman, A. E.; Rice, M. E.; Ritchard, N. T. Mechanisms of protein precipitation for two tannins, pentagalloyl glucose and epicatechin$_{16}$ (4→8) catechin (procyanidin). *J. Agric. Food Chem.* **1998**, *46*, 2590−2595.
(30) Zhu, Q. Y.; Zhang, A.; Tsang, D.; Huang, Y.; Chen, Z. Y. Stability of green tea catechins. *J. Agric. Food Chem.* **1997**, *45*, 4624−4628.
(31) Renugopalakrishnan, V.; Chandrakasan, G.; Moore, S.; Hutson, T. B.; Berney, C. V.; Bhatnagar, R. S. Bound water in collagen: evidence from Fourier transform infrared and Fourier transform infrared photoacoustic spectroscopic study. *Macromolecules* **1989**, *22*, 4121−4124.
(32) Robb, C. S.; Geldart, S. E.; Seelenbinder, J. A.; Brown, P. R. Analysis of green tea constituents by HPLC-FTIR. *J. Liq. Chromatogr. Relat. Technol.* **2002**, *25*, 787−801.
(33) Antonov, Y. A.; Wolf, B. A. Calorimetric and structural investigation of the interaction between bovine serum albumin and high molecular weight dextran in water. *Biomacromolecules* **2005**, *6*, 2980−2989.
(34) Van Buren, J. P.; Robinson, W. B. Formation of complexes between protein and tannic acid. *J. Agric. Food Chem.* **1969**, *17*, 772−777.
(35) Naczk, M.; Oickle, D.; Pink, D.; Shahidi, F. Protein precipitating capacity of crude canola tannins: effect of pH, tannin, and protein concentrations. *J. Agric. Food Chem.* **1996**, *44*, 2144−2148.
(36) Peters, T. J. *All about Albumin*; Academic Press: San Diego, CA, 1996.
(37) Ikeda, I.; Kobayashi, M.; Hamada, T.; Tsuda, K.; Goto, H.; Imaizumi, K.; Nozawa, A.; Sugimoto, A.; Kakuda, T. Heat-epimerized tea catechins rich in gallocatechin gallate and catechin gallate are more effective to inhibit cholesterol absorption than tea catechins rich in epigallocatechin gallate and epicatechin gallate. *J. Agric. Food Chem.* **2003**, *51*, 7303−7307.
(38) Beart, J. E.; Lilley, T. H.; Haslam, E. Plant polyphenols—secondary metabolism and chemical defense: some observations. *Phytochemistry* **1985**, *24*, 33−38.

Received for review February 28, 2007. Revised manuscript received April 20, 2007. Accepted April 26, 2007. This project is supported by the Center for Advanced Food Technology (CAFT) and in part by USDA-NRI.

JF070590L